

# Quantum transport and momentum conserving dephasing

Ivo Knittel, Florian Gabel and Michael Schreiber

*Institut für Physik, Technische Universität, D-09107 Chemnitz, Germany*

(August 3, 2018)

## Abstract

We study numerically the influence of momentum-conserving dephasing on the transport in a disordered chain of scatterers. Loss of phase memory is caused by coupling the transport channels to dephasing reservoirs. In contrast to previously used models, the dephasing reservoirs are linked to the transport channels between the scatterers, and momentum conserving dephasing can be investigated. Our setup provides a model for nanosystems exhibiting conductance quantization at higher temperatures in spite of the presence of phononic interaction. We are able to confirm numerically some theoretical predictions.

73.50.Bk, 73.20.Jc, 73.40.-c

## I. INTRODUCTION

The recently discovered jumps in the conductance of metallic nanowires and nanocontacts [1] have demonstrated impressively that quantum effects can dominate transport properties of small structures even at ambient temperature. This is generally explained by the lateral confinement which induces a rather large subband spacing of the transport modes of the conductor [2]. Within a single transport mode, phononic backscattering is considerably reduced because of the large amount of momentum transfer of  $p = 2\hbar k_F$  that has to be provided by a phonon. However, there remains the question whether the underlying picture of “ideal conductors” [3,4] is appropriate to describe e.g. metallic nanocontacts; if one insisted in a description in terms of ideal waveguides, one should account for the unavoidable imperfections of real systems like impurities or geometric deviations from the ideal-waveguides setup. The inclusion of coherent scattering centers in corresponding transport models leads, however, to the almost immediate loss of quantization of the conductance in the absence of some stabilizing mechanism.

An interesting question is whether dephasing, induced by phononic interaction, could provide such a mechanism: Interaction with longitudinal phonons, although not causing momentum transfer, can well be at the origin of dephasing which counteracts the weak localization of coherent backscattering. In this way, temperature could be helpful to

Typeset using REVTeX

re-establish quantization in this specific situation. For an investigation of this question transport models are needed which comprise elastic scattering as well as dephasing, while allowing for vanishing momentum transfer.

Many approaches to dephasing are based on reservoirs which destroy phase information in the same way as momentum information of passing electrons [5–9]; therefore, corresponding transport models are not suited for the investigation of the above discussed transport regime.

For the present study we have developed a model where coherent and incoherent scattering processes are conceptually separated. Coherent scattering is described by general elastic scatterers. We investigate single-mode transport through a one-dimensional chain of scatterers (Fig. 1).

Dephasing is induced using a common approach employing virtual electron reservoirs [5]. We have linked the reservoirs to the transport channels between elastic scatterers, exploiting the fact that electrons in transport channels automatically possess definite momenta. This seems to be the easiest way to implement momentum-selective coupling to a reservoir as has also been discussed by Datta [10]. Chemical potentials of such reservoirs thus correspond to occupation numbers of a local momentum distribution function as it occurs in the Boltzmann equation. This implies furthermore that emission from the reservoirs is uncorrelated with respect to the opposite direction of motion.

As depicted in Fig. 1, electrons absorbed by one of the two reservoirs between two scatterers are fed back incoherently into either the same transport channel or into the adjacent channel. In the latter case, they conserve their momentum as in the case of coherent propagation, while having, however, lost their phase memory. This permits us to investigate continuously different degrees of momentum conservation, from the case of

full momentum conservation to the case of momentum flip, independently from the dephasing strength itself.

Since only two scattering channels per scatterer are involved, our model is also efficient for numerical calculations which is of practical interest in order to cope with ensemble-averaging. It can also be easily extended towards multi-mode transport.

In the following section, we briefly generalize a method for the calculation of the scattering matrix of a composed system [11] towards the inclusion of dephasing reservoirs linked to “inner” channels. Section III reviews the involved characteristic lengths for phase, momentum and coherent localization and their relationship to the parameters of our model. Numerical results for the metallic and insulating regime are presented in section IV, and the influence of momentum-conserving dephasing on the transport is discussed.

## II. NUMERICAL APPROACH

We consider a one-dimensional chain consisting of  $N$  scatterers (see Fig. 1). Each scatterer has two channels and is described by its scattering matrix  $\mathbf{S}_k$  which relates linearly the outgoing to the incoming amplitudes at the scatterer. We have used the parametrization

$$\mathbf{S}_k = \begin{pmatrix} \sqrt{r_k} & i\sqrt{1-r_k} \\ i\sqrt{1-r_k} & \sqrt{r_k} \end{pmatrix}, \quad (1)$$

where  $r_k$  denotes the reflection probability of the scatterer  $k$ ,  $k = 1, \dots, N$ . A system of non-interacting scatterers would be described by a  $2N \times 2N$  scattering matrix  $\mathbf{K}$  containing the  $\mathbf{S}_k$  on its diagonal. Denoting the  $2N$ -tuples of incoming and outgoing amplitudes by  $c_+$  and  $c_-$ , respectively, we have  $c_- = \mathbf{K}c_+$ . For linked scatterers, we may distinguish between *external* and *internal* channels; external channels are con-

nected to the outside, e.g., the left and the right contact in the present case (channels 1 and  $2N$ ), while internal channels are interconnected: Amplitudes outgoing into internal channels are propagated to incoming amplitudes in internal channels, thus acquiring a phase shift  $\exp(ip)$  which may comprise either a simple geometric phase  $p = qd$  for a wave vector  $q$  and a distance  $d$ , or, generally also a magnetic phase  $\int A \cdot ds$  in presence of a vector potential  $A$ . This can be described by an operator  $\mathbf{P}$  which propagates internally outgoing amplitudes while annihilating externally outgoing amplitudes,  $c_{+, \text{int}} = \mathbf{P}c_-$ . Using the decomposition  $c_+ = c_{+, \text{int}} + c_{+, \text{ext}}$ , the relation

$$c_- = (\mathbf{K}^{-1} - \mathbf{P})^{-1} c_{+, \text{ext}} \quad (2)$$

is readily obtained [11]. The wanted scattering matrix  $\mathbf{S}$  of the composed system relates incoming to outgoing amplitudes in external channels, i.e.,

$$c_{-, \text{ext}} = \mathbf{S} c_{+, \text{ext}}; \quad (3)$$

it is thus given by

$$\mathbf{S} = \left( [(\mathbf{K}^{-1} - \mathbf{P})^{-1}]_{i,j} \right), \quad (4)$$

where the indices  $i, j$  label only the external channels.

The scattering matrix  $\mathbf{S}$  then yields the transmission matrix  $\mathbf{T}$  according to  $T_{ij} = |S_{ij}|^2$ ;  $T_{ij}$  is the transmission probability between the external channels  $j$  and  $i$ . The transmission matrix thus relates tuples of (dimensionless) outgoing and incoming currents,

$$I_- = \mathbf{T} I_+. \quad (5)$$

The associated incoming and outgoing currents are given by the squared moduli of the amplitudes in the external channels.

To incorporate dephasing in this approach, we assign a virtual reservoir to each

internal channel  $l$  and denote by  $\gamma_l$  the probability of getting absorbed by such a reservoir. The current into this reservoir is thus given by  $\gamma_l |c_-^{(l)}|^2$ . Current conservation then demands a corresponding loss term being accounted for also by the operator  $\mathbf{P}$ ; therefore, the assigned phase factor for coherent propagation of  $c_-^{(l)}$  has now to be multiplied by  $\sqrt{1 - \gamma_l}$ . For the considered chain it is given by e.g.

$$P_{ml} = \exp(ip_{ml}) \sqrt{1 - \gamma_l} \quad (6)$$

where  $m = l \pm 1$  for  $l$  even or  $l$  odd, respectively,  $p_{ml}$  denoting the phase for coherent propagation. Speaking in terms of currents, only a fraction  $1 - \gamma_l$  of the current outgoing in channel  $l$  is propagated coherently while a fraction  $\gamma_l$  is absorbed by the reservoir. In the following, we assume  $\gamma_l \equiv \gamma$  throughout for all internal channels  $l$  while we can formally assign  $\gamma_n = 1$  to external channels  $n$  which are fully absorbing; in this way, the virtual reservoirs are treated in the same way as the external contacts.

In the presence of the virtual reservoirs, the dimension of the transmission matrix  $\mathbf{T}$  has become larger and the matrix elements describing transmission from the virtual reservoirs are also needed. They can be obtained by replacing  $c_{+, \text{ext}}$  in Eq. 2 with  $c_{+, \text{int}} \sqrt{\gamma}$  where  $c_{+, \text{int}}$  is given by the  $l$ -th unit vector for virtual reservoir  $l$ . The squared moduli of  $c_-$  (multiplied by  $\gamma$  for internal channels  $i$ ) then yield the elements  $T_{il}$ , i.e., column  $l$  of  $\mathbf{T}$ .

The virtual reservoirs can now be used to introduce dephasing into the system [5]. For this purpose, electrons absorbed by the virtual reservoirs have to be re-emitted incoherently. The motion of electrons inside the considered system (see Fig. 1) can then be described as a Markovian process (see e.g. [7]): They are injected by the left contact, pass through virtual reservoirs and finally get absorbed by either the right or the left contact.

Adopting this point of view, we may renounce the notation of a chemical potential [5] which is convenient since we are interested in the total transmission only.

It is at the level of the transmission matrix where current conservation is imposed. We describe momentum conservation by a parameter  $\alpha$  ranging from 0 to 1; electrons absorbed by a reservoir between two scatterers in the chain conserve their momentum with probability  $\alpha$  while their momentum gets flipped with probability  $\bar{\alpha} = 1 - \alpha$  (see Fig. 1). The total transmission  $T$  is then given by

$$T = \quad (7)$$

$$T_{2N,1} + \sum_{l=1}^{N-1} [(T_{2N,2l+1}\alpha + T_{2N,2l}\bar{\alpha})T_{2l,1} \\ + (T_{2N,2l}\alpha + T_{2N,2l+1}\bar{\alpha})T_{2l+1,1}] \\ + \sum_{l,l'=1}^{N-1} (\dots) + \dots$$

as sum of transmission probabilities from the left to the right contact with 0, 1, ... intermediate passages through virtual reservoirs. This infinite series describing the random walk of the electrons can be summed analytically. We note that  $\mathbf{T}$  itself is symmetric due to time reversal invariance. Therefore, it is no surprise that the virtual reservoirs flip the momenta of absorbed electrons if the latter are fed back into the same channel; incoming and outgoing amplitudes in the same channel correspond to opposite momenta. Thus, our procedure of imposing current conservation only onto a pair of channels is well beyond the widely used description of Büttiker [5]; it is, however, covered by the more general approach of Datta [10].

### III. CHARACTERISTIC LENGTHS

The phase coherence length  $l_\Phi$  is given by the mean distance that an electron travels

coherently, i.e., the distance it conserves its phase. In order to relate it to the absorption probability  $\gamma$ , we consider the unperturbed system (without disorder, i.e., vanishing elastic backscattering) and obtain  $l_\Phi$  in units of the number of passed dephasing regions between the scatterers as

$$l_\Phi = \frac{\sum_{n=1}^{\infty} n(1-\gamma)^n}{\sum_{n=1}^{\infty} (1-\gamma)^n} = \frac{1}{\gamma}. \quad (8)$$

The mean free path  $l_m$  is the mean distance that an electron travels without being scattered, i.e., without momentum change. In order to obtain  $l_m$  in the unperturbed system, we consider the (incoherent) reflection probability  $\tilde{r}$  of a single dephasing region which is given by  $\tilde{r} = \bar{\alpha}\gamma$ . The resulting (dimensionless) resistance caused by a pair of corresponding reservoirs is  $\rho_0 = \tilde{r}/(1-\tilde{r})$ , which is additive for two incoherently coupled scatterers [5]. We now show that  $l_m := \rho_0^{-1}$  is a useful definition for the mean free path: For a chain of  $N$  dephasing areas, this yields a serial (four-probe) resistance of  $\rho = Nl_m^{-1}$ , and, because of  $\rho = (1-T)/T$ , a total transmission of

$$T = \frac{1}{1 + N/l_m}. \quad (9)$$

Equation 9 describes an Ohmic length dependence of the transmission; a section of length  $l_m$  contributes a resistance unit to the total resistance [10].

The effect of the coherent disorder can be described by the localization length  $l_\xi$ . We are extracting this length from the ensemble-averaged transmission of purely coherent systems, using the quantum scaling law of Anderson et al. (Ref. [12]),

$$\rho(N) = e^{N/l_\xi} - 1 \quad (10)$$

which differs from the well-known Landauer result [3] by a factor of 2. Ref. [12] predicts, assuming random phases between the scatterers, a localization length of the ensemble,

measured in number of scatterers, as

$$l_\xi = \langle t \rangle / \langle r \rangle \quad (11)$$

with the ensemble averages of the reflection and transmission probabilities  $r$  and  $t = 1 - r$  of a single scatterer. For our numerical investigation, we have employed a constant reflection probability  $r_k \equiv r$  and random phases  $p_{2k+1,2k} = p_{2k,2k+1} \in [0, 2\pi[$  (indicated by arcs in Fig. 1).

Performing numerical tests by logarithmically averaging up to  $10^4$  realizations of a purely coherent system ( $\gamma = 0$ ) consisting of up to  $N = 5 \times 10^4$  scatterers, we have found quite a good agreement with Eqs. 10, 11 (see Fig. 2). We have also tried a random box distribution with average  $r$  instead of constant reflection probability; this neither had an influence on the validity of Eq. 11, nor on the following results involving both coherent and incoherent processes.

#### IV. RESULTS

In order to investigate the interplay between the “microscopic” parameters  $r$ ,  $\gamma$  and  $\alpha$  and their counterparts, the characteristic lengths  $l_\xi$ ,  $l_\Phi$  and  $l_m$ , we distinguish between the “conducting” regime  $l_\Phi < l_\xi$  and the “insulating” regime where  $l_\xi < l_\Phi$ .

Two representative results are shown in Fig. 3 (left and right, respectively), where the computed ensemble-averaged total transmission is plotted as a function of the number of scatterers for dephasing which conserves, randomizes and flips momenta ( $\alpha = 1, 0.5$  and  $0$ , respectively). Transmission of the fully coherent system ( $\gamma = 0$ ) is similar to Fig. 2 (but not exactly the same due to the smaller number of averaged realizations).

The “conductor” can be thought of being composed of phase-coherent units which are linked incoherently, resulting in an Ohmic

length dependence of transmission. Since dephasing destroys localization, dephasing with full momentum conservation ( $\alpha = 1$ ) always enhances transmission when compared to a fully coherent system ( $\gamma = 0$  in Fig. 3).

The widely discussed case of simultaneous phase and momentum randomization [5] corresponds to  $\alpha = 0.5$ ; here, with increasing number of scatterers, transmission first drops due to incoherent backscattering, but there is always a certain length  $N$  such that the enhancement of transmission due to suppression of coherent localization outperforms the inelastic backscattering for systems larger than  $N$ . The absolute value of the transmission, however, already has become very small. Therefore, enhanced conductance due to dephasing can only be expected for a large degree of momentum conservation  $\alpha$ .

In the insulating regime, the dephasing rate, but also the backscattering rate are much smaller than in above discussed, “conducting” case. With  $l_\xi < l_\Phi$ , conduction properties are dominated by localization effects and cannot be understood in terms of incoherently coupled phase coherent units. Dephasing supports transmission significantly only for system sizes larger than  $l_\Phi$  when a deviation from the exponential dependence (described by Eq. 11) in the right diagram of Fig. 3 can be noticed. Finally, one would also expect an Ohmic behaviour for very large system sizes  $N \gg l_\Phi$ . Some enhancement of transmission in the insulating regime compared to the conducting regime appears but only for  $\alpha < 1$  (which can be seen comparing the two plots in Fig. 3). This is not unphysical: A large  $l_\Phi$  means small dephasing, which leads to a suppression of the quantum localization of the coherent system and thus increases transmission. For even larger dephasing (approaching the conducting regime), we get an increasing additional Ohmic resistance which finally causes the transmission to drop again (for  $\alpha < 1$ ).

In the insulator, the relative enhancement of the transmission for  $\alpha = 1$  compared to  $\alpha = 0.5$  or  $\alpha = 0$  is much smaller than for the case of the conductor, momentum conservation has less influence in this regime.

The importance of momentum conservation is best seen in Fig. 4 where the dependence of the transmission on the dephasing rate  $\gamma$  is plotted. Only for  $\alpha = 1$ , transmission increases monotonously with increasing  $\gamma$ . In the incoherent limit  $\gamma = 1$ , an Ohmic transport regime is reached with each single scatterer contributing the resistance  $l_\xi^{-1}$  (see Eqs. 9, 11), resulting in a transmission

$$T = 1/(1 + N/l_m + N/l_\xi). \quad (12)$$

For  $\alpha = 0.5$  and  $\alpha = 0$ , transmission passes through a certain maximum which has already been found for the case  $\alpha = 0.5$  in Ref. [5]; beyond this maximum, the additional resistance of the dephasing reservoirs causes a rapid decline.

In the following, we compare our numerical results (Figs. 3 and 4) to a formula which has been proposed by Band et al. [13] on the basis of ensemble averaged quantities. The dashed lines in Figs. 3 and 4 have been calculated using a slightly modified version of this formula.

In this approach, the transmission is given as

$$T = \frac{1}{1 + N/l_m + \rho_d(l_\xi, l_\Phi, N)} \quad (13)$$

with  $\rho_d$  being the resistance due to disorder for the case of infinite  $l_m$ . Equation 13 can be seen as a generalization of Eq. 9 towards the inclusion of disorder. The validity of Mathiessen's law is assumed in the sense that the two processes which cause momentum change, namely momentum flip by the reservoirs and coherent reflection by the scatterers, give independent contributions to the resistance. Note that they do not depend on  $l_\xi$  and  $\alpha$ , respectively. Surely, quantum resistance is generally not additive. However, the

range of validity of the approach of Ref. 13 is surprisingly large (see Fig. 4). Our numerical verification of the result of Band et al. shows excellent agreement. A pre-requisite for this is our dephasing model, which allows for momentum conservation.

In the presence of dephasing (for finite  $l_\Phi^{-1}$ ),  $\rho_d$  can be built up recursively from the resistance of the purely coherent case,  $\rho_c(x; l_\xi) = e^{x/l_\xi} - 1$ , and from the probability density  $P(x; N, l_\xi, l_\Phi)$  for an electron to travel coherently a distance  $x$  within the disordered wire and to lose phase information at position  $x$  by a dephasing event. Both  $\rho_c(x; l_\xi)$  and  $P(x; N, l_\xi, l_\Phi)$  are ensemble averages. In the case  $l_\Phi < N$ , Band et al. obtain

$$\rho_d(N, l_\xi, l_\Phi) = \frac{N \int_0^N P(x; N, l_\xi, l_\Phi) \rho_c(x; l_\xi) dx}{\int_0^N x P(x; N, l_\xi, l_\Phi) dx}. \quad (14)$$

Since both localization and dephasing processes lead to an exponential length decay of the probability,

$$P(x; N, l_\xi, l_\Phi) = l_\lambda^{-1} e^{-x/l_\lambda} + e^{-N/l_\lambda} \delta(x - N), \quad (15)$$

with  $x \in [0, N]$ , is a plausible choice, with a disorder modified phase coherence length  $l_\lambda(l_\xi, l_\Phi)$ . In their original work, Band et al. have proposed

$$l_\lambda^{-1} = l_\Phi^{-1} + 2l_\xi^{-1}; \quad (16)$$

however, in more recent work [14,15], a phase coherence length in a disordered quantum wire is defined in a similar context as

$$l_\lambda^{-1} = l_\Phi^{-1} + l_\xi^{-1}. \quad (17)$$

Our numerical results are better described using Eq. 17.

Equation 13 has been employed for Figs. 3 and 4. This gives a rather good agreement, except for the case  $l_\Phi > l_\xi$  (right diagram of Fig. 3) where the contribution of inelastic backscattering ( $\alpha = 0$ ) to the resistance

is slightly underestimated; Mathiessen's law may thus not be valid in this regime.

For the interesting case of enhanced dephasing rates, Eq. 13 can be used to estimate the achievable change of transmission compared to purely coherent transmission. The maximum enhancement  $\Delta T$  is obtained for  $l_\Phi = 0, l_m = \infty$ ; using Eqs. 10 and 12, we obtain with  $\chi := N/l_\xi$

$$\Delta T = 1/(1 + \chi) - e^{-\chi}. \quad (18)$$

This yields a maximum  $\Delta T_{\max} \approx 0.20$  for  $\chi_{\max} \approx 2.51$ .

## V. CONCLUSIONS

We have presented a model of general scatterers which allows us to investigate quantum transport through a disordered system in the presence of dephasing with a tunable degree of momentum conservation. We obtained the rather obvious result that momentum conservation is essential if dephasing is to enhance transmission. From Fig. 3, it is evident that support for a quantized conductance by dephasing can be expected in the regime  $l_\Phi < N \approx l_\xi$ .

Our numerical results have been compared to a general but heuristic picture developed in Ref. [13] which is based on the validity of Mathiessen's rule and an ad hoc assumption for a probability density  $P(x; N, l_\xi, l_\Phi)$ ; it is not derived from a microscopic theory, but gained its plausibility from its validity in various limiting cases. Furthermore, it is not evident that average quantities as  $\rho_c(x)$  and  $P(x; N, l_\xi, l_\Phi)$  can be employed in a recursive formula for the transmission, since sample averaging is not a simple commutative operation and since there are different types of averaging procedures which often proved intuition wrong in the past [12]. Therefore, it is rather surprising that Eq. 13 gives a good fit of our data, except for the strongly insulating regime,  $l_\xi \ll l_\Phi \ll N$ .

However, while the previously discussed approach by Band et al. yields a good agreement for the ensemble-averaged transmission, it cannot predict fluctuations. For the investigation of conductance quantization effects, it is highly desirable to describe a single system or at least the applicability of results for ensemble averages to a particular realization. Here, our general quasi-microscopic model provides a helpful tool. In nanosystems exhibiting conductance quantization, elastic backscattering is reduced (but not absent) because of the larger subband spacing which is itself induced through the geometrical confinement. At higher temperatures, one has to account for phononic interaction, notably with longitudinal phonons, leading to dephasing but not inelastic backscattering. As mentioned in the introduction, one can describe this situation by momentum-conserving dephasing which was not included in previous models. While we found an excellent agreement with the approach of Ref. 13 over a wide range, the domain of applicability to (quasi-)quantization in nanosystems would be for  $N \leq l_\Phi < l_\xi$ . Work along these lines is in progress. An advantage compared to an heuristic approach is that we are able to investigate also fluctuations and single realizations.

## REFERENCES

- [1] J. L. Costa-Krämer, N. García, H. Olin, Phys. Rev. Lett. **78**, 4990 (1997); J. L. Costa-Krämer, N. García, P. García-Mochales, P. A. Serena, Surf. Sci. Lett. **342**, L1144 (1995)
- [2] H. van Houten, C. Beenakker, Physics Today **7** (July), 22 (1996)
- [3] R. Landauer, Philos. Mag. **21**, 863 (1970)
- [4] R. Landauer, Z. Phys. B **68**, 217 (1987); R. Landauer, J. Phys.: Condens. Matter **1**, 8099 (1989)
- [5] M. Büttiker, Phys. Rev. B **33**, 3020 (1986)
- [6] J. L. D'Amato and H. M. Pastawski, Phys. Rev. B **41**, 7411 (1990)
- [7] H. M. Pastawski, Phys. Rev. B **44**, 6329 (1991)
- [8] M. J. McLennan, Y. Lee, S. Datta, Phys. Rev. B **43**, 13846 (1991)
- [9] G. Burmeister, K. Maschke, M. Schreiber, Phys. Rev. B **47**, 7095 (1993)
- [10] S. Datta, "Electronic transport in mesoscopic systems", Cambridge University Press, Cambridge 1993
- [11] F. Gagel, K. Maschke, Phys. Rev. B **49**, 17170 (1994)
- [12] P. W. Anderson, D. J. Thouless, E. Abrahams, D. S. Fisher, Phys. Rev. B **22**, 3519 (1980)
- [13] Y. B. Band, H. U. Baranger, Y. Avishai, Phys. Rev. B **45**, 1488 (1992)
- [14] K. Maschke, M. Schreiber, Phys. Rev. B **49**, 2295 (1994)
- [15] R. Hey, K. Maschke, M. Schreiber, Phys. Rev. B **52**, 8184 (1995)

## FIGURES

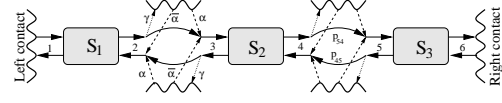


FIG. 1. A chain consisting of  $N = 3$  scatterers  $S_1$ ,  $S_2$  and  $S_3$ . Channels 1 and 6 link the system to the left and right contact. Electrons outgoing from the scatterers in inner channels 2–5 may travel coherently or incoherently between the scatterers. When traveling coherently, they acquire a phase shift  $p$  (indicated by arcs). Alternatively, they may get absorbed (dotted arrows, probability  $\gamma$ ) between the scatterers by reservoirs (wavy lines). From the reservoir they are re-emitted (dashed arrows) either with same momentum (probability  $\alpha$ ) or inversed momentum (probability  $\bar{\alpha} = 1 - \alpha$ ).

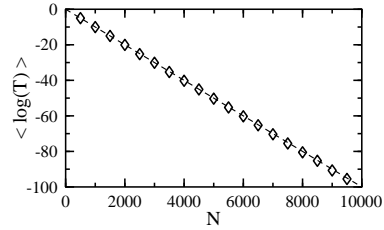


FIG. 2. Transmission of a chain of  $N$  coherently coupled scatterers with backscattering probability  $r = 0.01$ . Each point is obtained by logarithmically averaging  $10^4$  realizations. The dashed line corresponds to Eq. 10 with a localization length  $l_\xi = 99 = (1 - r)/r$ .

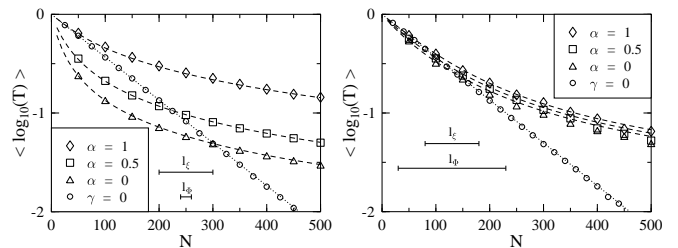




FIG. 3. Transmission as function of the number of scatterers for three different degrees of momentum conservation  $\alpha$ . The elastic backscattering probability is  $r = 0.01$  corresponding to a localization length  $l_\xi = 99$ . The left diagram is calculated for dephasing probability  $\gamma = 0.05$ , the right diagram for  $\gamma = 0.005$ . Each point is obtained by logarithmically averaging 1000 realizations. Also indicated is the transmission of the coherent system ( $\gamma = 0$ ). The dashed and dotted lines indicate solutions of Eq. 13 and Eq. 11, respectively.

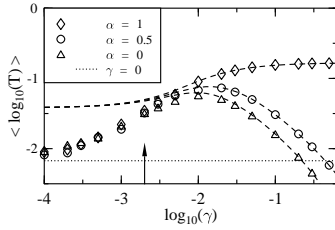


FIG. 4. Total transmission for a chain of  $N = 500$  scatterers as a function of the dephasing parameter  $\gamma$  for three different degrees of momentum conservation  $\alpha$ . The elastic backscattering probability is  $r = 0.01$  corresponding to a localization length  $l_\xi = 99$ ; each point is obtained by logarithmically averaging 1000 realizations. The lines are obtained from Eq. 13 which is applicable for  $\gamma > 1/N$  (indicated by the arrow).